Volume 38 | Number 8 | August 2014 | Pages 3305–4008

NJC

New Journal of Chemistry

www.rsc.org/njc

A journal for new directions in chemistry

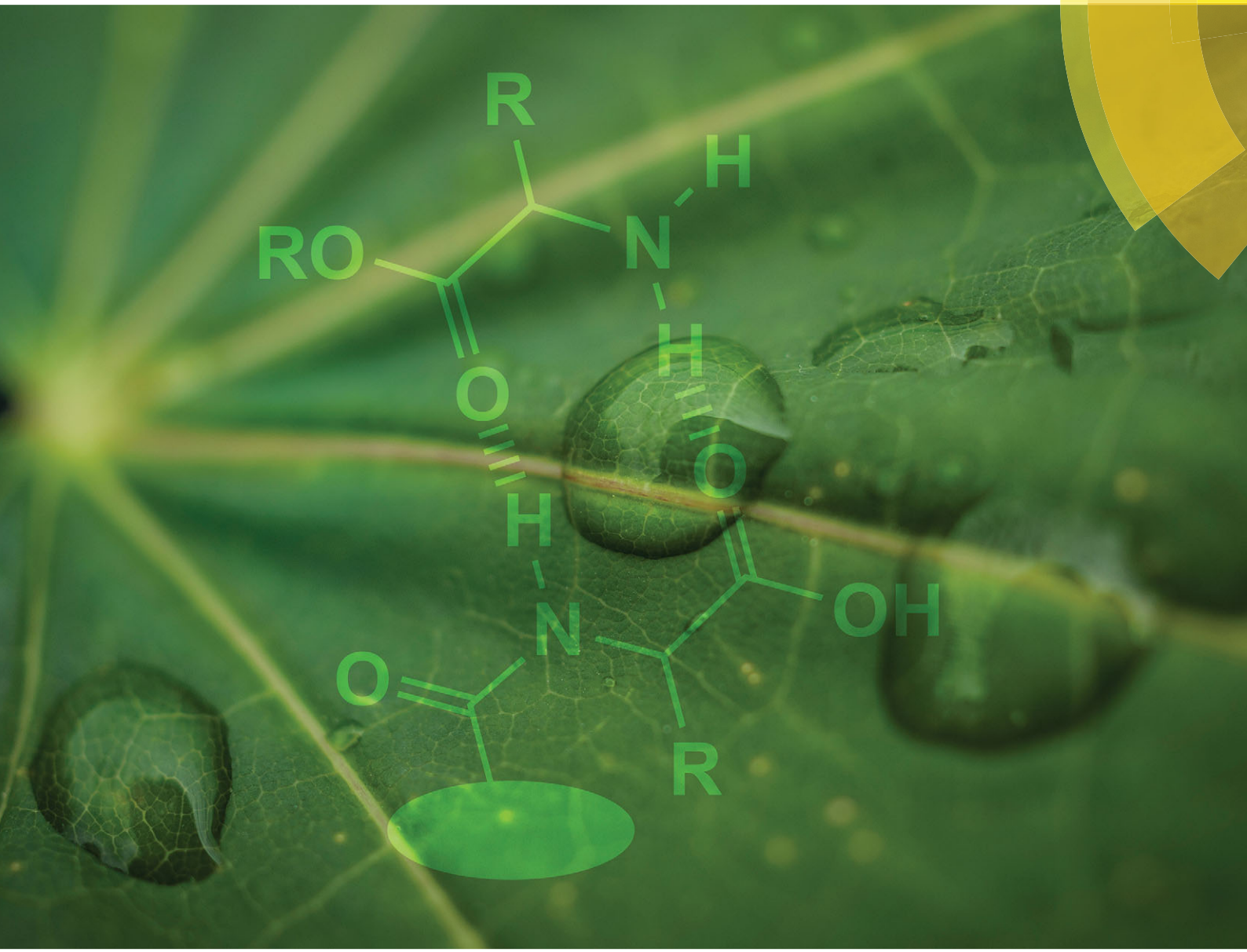

ISSN 1144-0546

ROYAL SOCIETY OF CHEMISTRY

PAPER

M'hamed Chahma *et al.*

Characterization of phenomena occurring at the interface of chiral conducting surfaces

cnrs

NJC

PAPER

Characterization of phenomena occurring at the interface of chiral conducting surfaces

Cite this: *New J. Chem.*, 2014, **38**, 3379

M'hamed Chahma,* Christopher D. McTiernan and Sara A. Abbas

The ability of the chiral electrode based on L-leucine functionalized terthiophene (poly(**1**)-Pt) to recognize and detect biomolecules has been studied as a function of hydrogen bonding between the chiral surface and a free L-leucine methyl ester. We characterized electrochemically the formation of hydrogen bonds by cyclic voltammetry (CV). The results show that the capacitive current of the chiral electrode poly(**1**)-Pt decreased by 30% due to hydrogen bonding between the chiral electrode and the free added L-leucine methyl ester. The origin of the hydrogen bonds on poly(**1**)-Pt has been confirmed by attenuated total reflection Fourier transform infrared (ATR-FTIR) using trifluoroacetic acid (CF_3COOH) as free H-bonding species. The ATR-FTIR spectrum exhibits functionalities of free CF_3COOH that form hydrogen bonds with the chiral conducting surface of poly(**1**)-Pt. Due to the insolubility of poly(**1**), NMR studies were performed on the parent monomers. The chemical shift of the amide proton in the ^{1}H-NMR of the L-leucine functionalized terthiophene (**1**) shifted after addition of L-leucine methyl ester. Similar trends were observed for the carboxylic carbonyl of L-leucine methyl ester-terthiophene **2** in the ^{13}C-NMR. In addition to the change in the ^{13}C chemical shift, there is a considerable change in the spin–lattice relaxation time of the carbonyl carbon in **2** due to the formation of hydrogen bonds between the –COOH of **2** and the imidazole.

Received (in Porto Alegre, Brazil) 29th March 2014,
Accepted 14th May 2014

DOI: 10.1039/c4nj00489b

www.rsc.org/njc

Introduction

Surface modification allows for the immobilization of a variety of organic and bioorganic molecules such as DNA,[1,2] proteins,[3,4] peptides[5,6] and lipids[7] on conducting and semi-conducting surfaces, leading to several applications in different research areas, including biosensors[8–11] and biomaterials.[12,13] Being able to control functionalities on conducting surfaces can help tune the chemical and electrochemical properties of the modified surfaces, thereby affecting the detectability of immobilized molecules on such surfaces.

Many methods used to immobilize biomolecules directly or indirectly on conducting and/or semi-conducting surfaces have been described. For instance, self-assembled monolayers (SAMs) are commonly used to modify gold (Au) surfaces.[14–16] *Via* reduction of thiols,[17,18] disulfides[19,20] or sulfenyl chlorides,[21,22] a variety of organic and bioorganic molecules have been immobilized on gold surfaces to form S–Au bonds. Moreover, by reducing the aryl diazonium salts or oxidizing aromatic amines, other organic molecules have also been grafted on glassy carbon (GC) electrodes *via* formation of carbon–carbon (C–C)[23–26] and carbon–nitrogen (C–N)[27,28] bonds.

Another strategy has been reported for surface modification which involves the immobilization of organic/bioorganic molecules by trapping electroactive polymers such as polythiophene, polyaniline, and polypyrrole.[29,30] In this method, the attachment of molecules involves a covalent bond between the biomolecule and the deposited polymer *via* electrochemical oxidation on platinum (Pt) electrode. For example, a glucose-biosensor based on the electrochemical deposition of polythiophenes bearing pendant glucose oxidase has been developed.[31] In other instances, polythiophenes have been tuned into electronic transducers by covalently binding them to bioreceptors such as biotin with an avidin motif.[32–34]

Polythiophenes bearing chiral centers have also been prepared either by electrochemical[35,36] or chemical oxidation using $FeCl_3$ as oxidizing agent.[37–39] The resulting chiral polymer were stable and it was shown that the stereochemistry of the chiral center did not affect the absorption properties.

Moreover, L-cysteine functionalized polythiophene films have been deposited on metallic plate using spin-casting and spin-coating techniques. The chirality of these films and the overall formation of chiral polymer aggregation can be tuned through control of the applied electrical field and solvent evaporation.[40,41]

For recognition purposes, luminescent chiral conjugated polythiophenes have demonstrated interesting optical sensing properties toward detection of peptides[42] and proteins.[43]

The immobilization of organic/bioorganic molecules on electroactive materials displays advantages such as the ability to be regenerated by controlling the thickness of the deposited film layers. These layers could be used as an interface between

Department of Chemistry & Biochemistry, Laurentian University, Sudbury, ON, P3E 2C6, Canada. E-mail: mchahma@laurentian.ca; Fax: +1-705-675-4844; Tel: +1-705-675-1151 (ext. 2213)

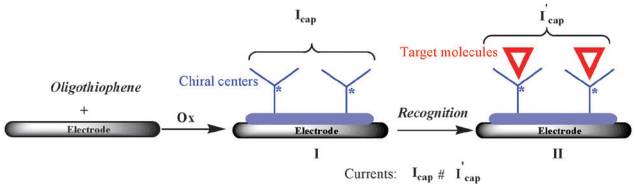

Chart 1 Discrimination of biomolecules using chiral electrodes.

biomolecular probes and electrode surfaces, which can further facilitate immobilization and sensing of the desired molecules. Recently, we prepared several chiral conducting surfaces based on alanine, proline and leucine-functionalized polythiophenes *via* electrochemical oxidation of their corresponding thiophene monomers.[44–46] These chiral surfaces exhibit excellent electrochemical stability in doped and undoped states, and contain several chiral centers where hydrogen bond interactions can occur with free biomolecules.

Herein, we present the preparation of chiral conducting surfaces (**I**) and the characterization of their interactions with free target molecules in solution (**II**). In cyclic voltammetry, the resulting capacitive current I_{cap}' of surface **II** is decreased as opposed to I_{cap} of surface **I** (Chart 1). The shifts observed in the capacitive currents are due to the formation of the hydrogen bonds between the chiral surface and the free amino acids. Moreover, we present ATR-FTIR and NMR results that validate the inference that hydrogen bonds are formed on the chiral conducting surfaces.

Experimental section

Generalities

Unless stated otherwise, all reactions and manipulations were carried out in an argon atmosphere. Glassware was oven-dried at 100 °C for 24 h prior to use. Solvents were dried using an activated molecular sieve (4 Å, 24 hours at 100 °C). All reagents were purchased from commercial sources and used as received. ^{1}H-proton (^{13}C-carbon) NMR spectra were recorded on a 500 (125) MHz NMR spectrometer.

Electrochemistry

The electrochemical experiments (iR compensations applied) were performed using a potentiostat at room temperature (22 ± 2 °C). Voltammetric measurements were performed in acetonitrile (ACN) containing 1 M of *n*-Bu_4NPF_6. A platinum electrode (diameter 1.6 mm) was the working electrode, polished on alumina before use. Platinum wire was the auxiliary electrode and silver wire the reference electrode. All oxidation peak potentials are reported *versus* an internal reference ferrocene/ferrocenium redox (E^0 = 0.390 V *vs.* AgCl/Ag, E^0 = 0.350 V *vs.* SCE).

Bulk electrolyses were performed using controlled potential in a cell with one compartment using a platinum plate (1.5 cm^2) and ITO (Indium Tin Oxide) as the anode and cathode, respectively. The imposed potential for the electrolysis of compound 1 is 1.3 V (*vs.* AgCl/Ag). The capacitive current was measured using cyclic voltammetry and data analysed with Microsoft Excel. In order to find the total charge, the total area between the forward and reverse curves was calculated using the method of Riemann summation[47] and then divided by the scan rate (mV s^{-1}).

^{1}H-NMR study of 1 with free L-leucine methyl ester (LeuOMe)

The NMR samples were prepared by dissolving 15 mg (51 mM) of compound **1** in 0.7 mL of deuterated DMSO-d_6. Then, 1 equivalent (6.5 mg, 51 mM) and 2 equivalents (13 mg, 101 mM) of LeuOMe ester were added, respectively. All recorded spectra are based on 128 scans.

^{13}C-NMR study of 2′ with free imidazole

The NMR samples were prepared by dissolving 15 mg (56 mM) of compound **2′** in 1 mL of deuterated DMSO-d_6. Then, 1 equivalent (4 mg, 56 mM) of imidazole was added to the solution. Recorded spectra are based on 256 scans.

^{13}C-NMR study of 2 with free imidazole

The NMR samples were prepared by dissolving 15 mg (59 mM) of compound **2** in 1 mL of deuterated DMSO-d_6 and the recorded spectra are based on 256 scans. Then, 1 (4 mg, 59 mM) equivalent of imidazole was added to the solution. Recorded spectra are based on 256 or 512 scans.

ATR-FTIR measurements

0.01 M of 4-methyl-2-(2-[2,2,5,2]terthiophene-3-yl)-[acetylamino]-pentanoic acid (**1**) was electropolymerized on the platinum electrode (1.5 cm^2) using controlled potential electrolysis. The imposed potential for the electrolysis was 1.3 V (*vs.* AgCl/Ag). After the electropolymerization, poly(**1**)-Pt was removed from the solution and washed 5 times with ACN, and 3 times with CH_2Cl_2 to remove all free monomers. The modified electrode poly(**1**)-Pt was dried in air and the ATR-FTIR spectrum was recorded. The electrode was then incubated for 5 minutes in a solution of ACN containing 20 mg of trifluoroacetic acid (CF_3COOH). Thereafter, the electrode was washed 5 times with ACN and 5 times with CH_2Cl_2 to ensure that all free CH_3COOH was removed. The electrode was again dried and ATR-FTIR spectrum recorded. ATR-FTIR spectra were collected using a Bruker Optics Infrared Microscope with ATR objective and Ge crystal. The resolution of the spectrometer was 4 cm^{-1} and the spectrum was collected with 500 scans. The spectrometer was equipped with a MCT detector cooled with liquid nitrogen. The atmospheric compensation and baseline corrections were performed with OPUS computer software.

Results and discussions

In order to investigate phenomena occurring at the surface of chiral conducting surfaces based on terthiophenes bearing amino acids, several L-leucine functionalized oligothiophenes (**1**, **1′**, **2**, **2′**) have been prepared according to a procedure previously described (Scheme 1).[48]

4-Methyl-2-(2-[2,2;5,2]terthiophene-3-yl)-[acetylamino]-pentanoic acid (**1**) was deposited on platinum electrode *via* electrochemical oxidation using repeated cyclic voltammetry scans beyond its

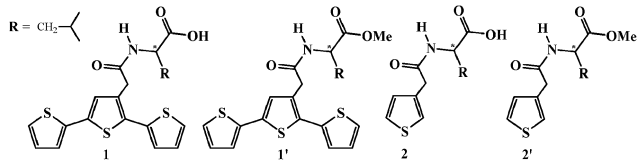

Scheme 1 L-Leucine functionalized oligothiophenes.

oxidation potential. Fig. 1A shows an increase in the peak current after each successive scan, which indicates the formation of the polymer on the electrode surface. Moreover, a second peak appears at a lower oxidation potential than the monomer, which corresponds to the oxidation potential of the deposited polymer.[49,50]

After polymer formation, the electrochemical stability of poly(**1**)-Pt was studied by applying 100 CV cycles at constant scan rate. Fig. 1B shows that there is no change or degradation of their electrochemical behaviors, which demonstrates excellent stability of the polymer on Pt electrode.[51]

Fig. 2A–C show the differences in the capacitive currents observed after addition of 0.1, 1 and 5 mM of free LeuOMe. After 30 min, the capacitive current decreases and reaches a plateau for all concentration of LeuOMe (Fig. 2A′–C′). The maximum plateau was found to be 30% of the initial capacitive current (current of the chiral electrode in the absence of free amino acid) for **1** and 5 mM of LeuOMe, which shows that all pending chiral centers in poly(**1**)-Pt surface, which are susceptible to form hydrogen bond have been saturated. The 0.1 mM of LeuOMe was not enough to saturate the chiral surface poly(**1**)-Pt with hydrogen bonds, which may explain the 20% of the plateau observed in the capacitive current.

Several films of different thickness (*i.e.* different initial capacitive current I_{cap}) have been prepared and used to probe free Leu-OMe at concentration of 1 and 5 mM. In all cases the observed changes in capacitive current are similar, with the initial capacitive current decreasing by roughly 30% upon addition of analyte. This is however not unexpected considering only the outermost layer of the polymer is capable of forming hydrogen bonds with the analyte, and therefore polymer thickness should not have effect on the measurement.

The capacitive current depends on the concentration of the supporting electrolyte.[52] As hydrogen bonds are formed on the chiral conducting surfaces after addition of free LeuOMe, supporting electrolyte ions are trapped and cause a decrease in the capacitive current. Similar behavior has been observed for polybithiophenes bearing oligonucleotides.[53,54]

Due to the limited solubility of leucine in organic solvents, its methyl ester LeuOMe has been used for the hydrogen bond interaction studies. The presence of the ester group on LeuOMe weakens the hydrogen bond formation, which may explain its slow adsorption on poly(**1**)-Pt surface (Scheme 2).

It is well known that –CONH and –COOH functionalities are involved in the hydrogen-bond formation in proteins. Such interactions are strong and play an important role in the biological activities of proteins.[55] Poly(**1**)-Pt displays a chiral center such as leucine where hydrogen bonds can occur. By blocking the COOH, the extent of hydrogen bonds formed on the surface of the chiral electrode decreases. For this reason, 4-methyl-2-(2-[2,2;5,2]terthiophene-3-yl)-[acetylamino]-pentanoic acid methyl ester (**1′**) was electropolymerized using cyclic voltammetry. The capacitive currents for poly(**1′**)-Pt were measured before and after addition of LeuOMe (Fig. 3). After 30 minutes the capacitive current of poly(**1′**)-Pt in the presence of 1 mM (5 mM) of LeuOMe decreased only by 5%, whereas the capacitive current of poly(**1**)-Pt decreased by 30%.

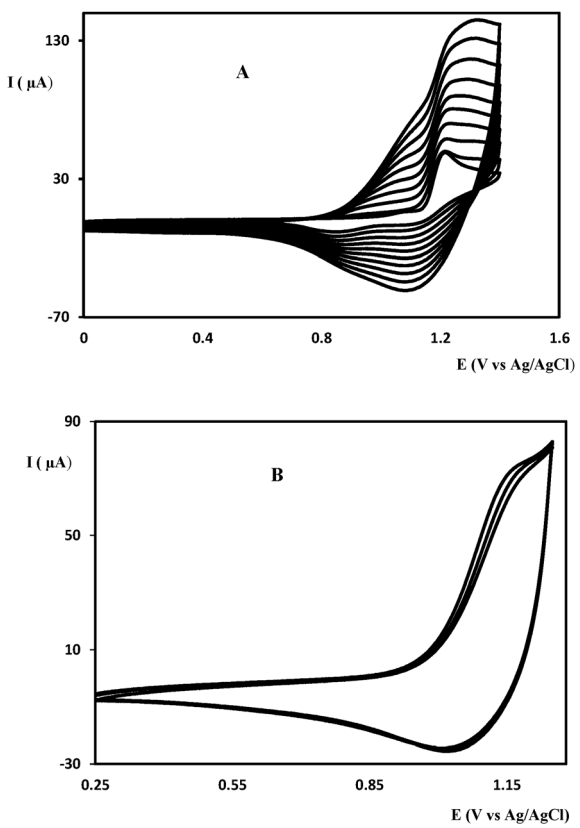

Fig. 1 Electropolymerization of **1** (A) and stability of poly(**1**)-Pt over 100 scans (B).

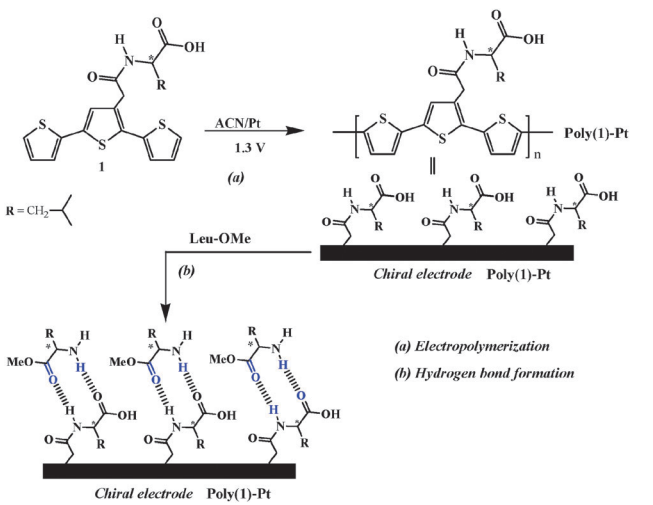

Scheme 2 Chiral conducting surfaces (poly(**1**)-Pt).

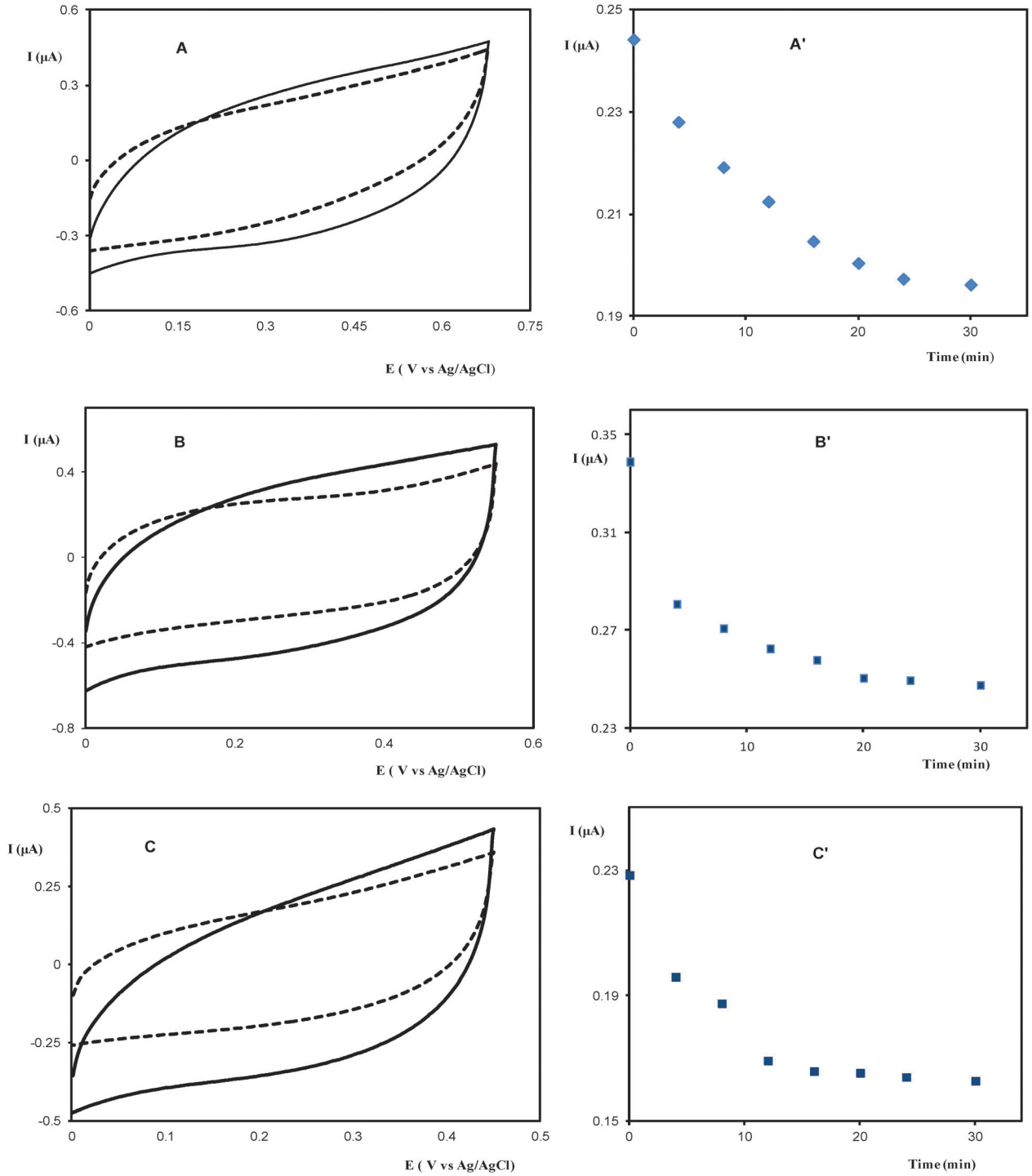

Fig. 2 Capacitive current of poly(**1**)-Pt (solid line: left) at different concentrations of LeuOMe (dash line: right) and variation of the capacitive current with time (right). The capacitive current was determined for the oxidation process. The capacitive current was measured before and after addition of LeuOMe. For every concentration of LeuOMe, The capacitive current of poly(**1**)-Pt was measured from 0 min to 30 min after addition of LeuOMe.

Since the methyl ester group blocks the active site of the chiral electrode, this must limit the formation of hydrogen bonds on poly(**1**′)-Pt surface.

ATR-FTIR was used to probe the hydrogen bond formation between the chiral conducting surface poly(**1**)-Pt and another organic molecule carrying specific functionalities.[56]

For ATR-FTIR measurements, poly(**1**)-Pt was prepared by controlled potential electrolysis at 1.3 V *vs.* (Ag/AgCl) onto a platinum plate. Poly(**1**)-Pt surfaces prepared either by electrolysis or by CV scans are identical and have the same electrochemical, and optical properties. ATR-FTIR studies were firstly carried out to probe the adsorption of free LeuOMe on poly(**1**)-Pt.

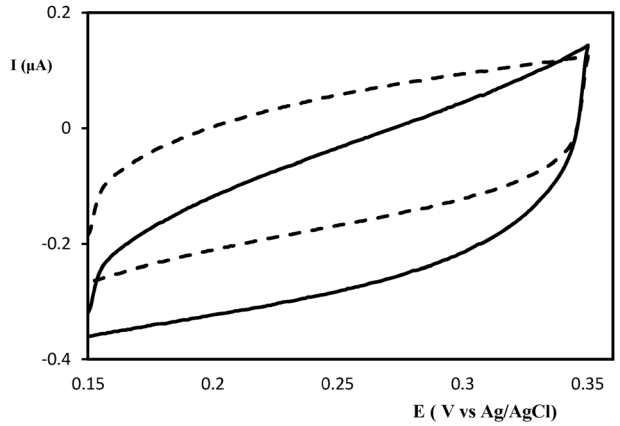

Fig. 3 The capacitive current of poly(**1**′)-Pt before (solid line) and after (dash line) addition of LeuOMe (1 mM).

However, no changes were observed in the ATR-FTIR spectrum of poly(**1**)-Pt after 30, 60 and 120 minutes incubation in a LeuOMe solution.

Trifluoroacetic acid (CF_3COOH) has been chosen because its IR spectrum exhibits strong stretchings at 1188 cm^{-1} ($-CF_3$) and 1774 cm^{-1} (–COOH).[57] ATR-FTIR spectrum has been recorded after electropolymerization of **1** on Pt electrode in order to form a chiral surface poly(**1**)-Pt with pendant chiral center (leucine). Fig. 4 (dash line) shows the ATR-FTIR characterizations of the doped chiral conducting surface poly(**1**)-Pt, which are summarized in Table 1.

Poly(**1**)-Pt was then incubated in a solution of CF_3COOH for a few minutes and the ATR-FTIR spectrum recorded (Fig. 4, full line). Although no significant shifts were observed for the amide and the carboxylic acid of poly(**1**)-Pt (immersed in a solution of CF_3COOH), two bands emerged at 1162 cm^{-1} and 1782 cm^{-1}, corresponding to $-CF_3$ and –COOH groups of CF_3COOH (Fig. 4).[57] The presence of bands characteristic to CF_3COOH come from the strong hydrogen bond interactions between CF_3COOH and the chiral surface poly(**1**)-Pt. Furthermore, in the presence of CF_3COOH, poly(**1**)-Pt was reduced and turns orange (undoped state). During the reduction process, the counter ion PF_6^- is expulsed, which explains the decrease in the intensity of the PF_6^- band at 846 cm^{-1} observed

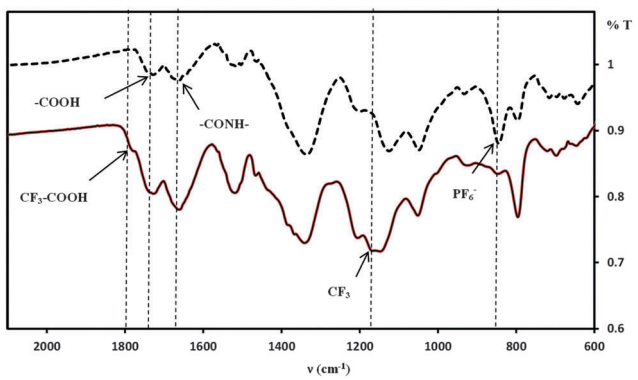

Fig. 4 TR-FTIR of poly(**1**)-Pt (dash line) and poly(**1**)-Pt/CF_3COOH (solid line).

Table 1 ATR-FTIR characteristics of poly(**1**)-Pt and poly(**1**)-Pt/CF_3COOH

υ (cm^{-1})	Poly(**1**)-Pt	Poly(**1**)-Pt/CF_3COOH
1782	—	**CO(CF_3COOH)**
1730	CO(COOH)	CO(COOH)
1662	CO(CONH)	CO(CONH)
1336	C═C	C═C
1162	—	**CF_3**
846	PF_6^-	PF_6^-

in Fig. 4 (line).[58] The ATR-FTIR characterizations of poly(**1**)-Pt/CF_3COOH are summarized in Table 1.

Since poly(**1**) is insoluble in organic solvents, monomer **1** has been utilized as a model of the chiral surfaces to study hydrogen bond formation between the electroactive oligothiophene monomers and free LeuOMe by ^{1}H-NMR.

Fig. 5 shows the chemical shift of N–H (amide) group changed from 8.35 ppm to 8.50 ppm in terthiophene **1** after addition of 1 equivalent of LeuOMe. Moreover, the chemical shifts of the thiophene aromatic protons remain unchanged before and after addition of LeuOMe, which indicates that the hydrogen bond is formed between the amide group in the chiral surface and the carboxylate group of LeuOMe. The coupling constant of the amide proton (doublet) of **1** increased from 7 Hz to 8 Hz.

^{13}C-NMR has also been used to observe the interaction between the acid of the leucine attached to the thiophene moiety and a free organic molecule such as imidazole. The ^{13}C shifts of –CONH and –COOMe in compound **2**′ are 170.1 and 173.3 ppm, respectively (Table 2). In the presence of 1 equivalent of imidazole, the ^{13}C of the carbonyls remains constant (Fig. 6), indicating no hydrogen bond formation between compound **2**′ and imidazole.

However, the ^{13}C chemical shift of –COOH, 174.1 ppm in compound **2** shifted by 0.3 ppm (174.4 ppm) due to H-bonding in the presence of 1 equivalent of imidazole (Fig. 6), also summarized in Table 2 and depicted in Scheme 3.

The ^{13}C peak intensity of –COOH in compound **2** decreased in the presence of imidazole. After 512 scans, the peak of –COOH starts to recover. But the intensity of the –COOH is much lower

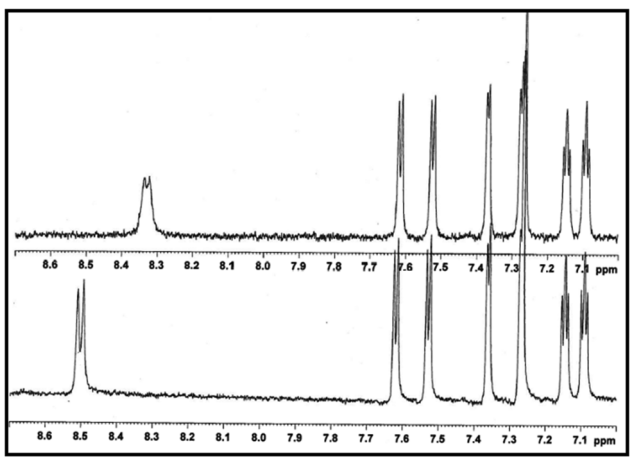

Fig. 5 ^{1}H-NMR of **1** in the absence (top) and in the presence (bottom) of one equivalent of LeuOMe.

Table 2 ^{13}C chemical shift of the carbonyl carbons in **2** and **2′**

Compound	δ_{CONH} (ppm)	δ_{COOH} (ppm)
2′	170.1	173.3
2′ + imidazole	170.1	173.3
2	169.8	174.1
2 + imidazole	169.8	**174.4**

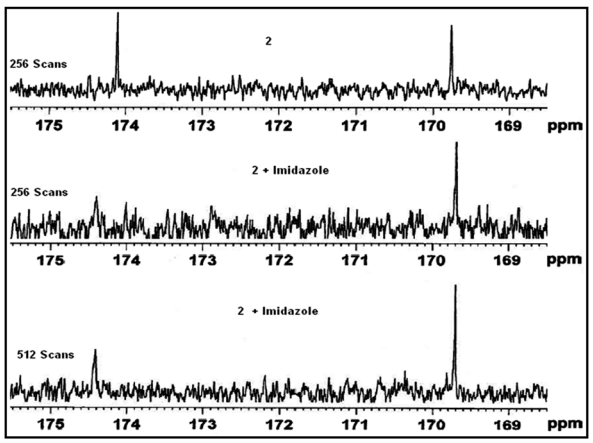

Fig. 6 ^{13}C-NMR of **2** in the absence and in the presence of one equivalent of imidazole.

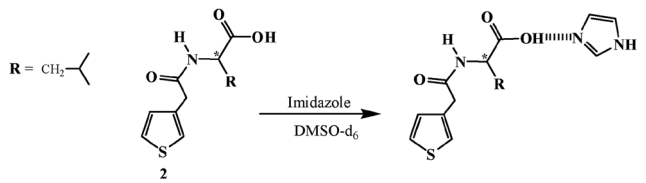

Scheme 3 Interactions between **2** and imidazole in DMSO-d_6.

than the intensity of the amide carbonyl peak (Fig. 6, 512 scans). Since the intensity of NMR signals depends of the relaxation time, we conclude that the formation of hydrogen bond between **2** and imidazole affects the longitudinal relaxation time (spin–lattice relaxation time) of the –COOH.[59,60] Similar trends have been observed in spin–lattice relaxation time of the carbonyl for the epoxy resin (ER) in the presence of poly(ε-caprolactone)(PCL) using different fractions of ER/PCL.[61]

Summary

Terthiophene bearing L-leucine monomer was oxidized electrochemically using cyclic voltammetry to deposit thin films with specific chirality (chiral electrode) on platinum electrode. The chiral electrode displays excellent stability and adhesive properties on the Pt surfaces. In order to test the recognition ability of these electrodes, the capacitive current of the chiral electrode has been measured in the absence and presence of a free amino acid such as L-leucine methyl ester (LeuOMe). We found that the capacitive current of the chiral electrode decreases by 30% after addition of 1 or 5 mM of LeuOMe. The change observed in the capacitive current is attributed to the formation of hydrogen bonds between the chiral surfaces and the free amino acids in solution. Such hydrogen bond formation between the chiral electrode and CF_3COOH was confirmed by ATR-FTIR. Since poly(**1**) is insoluble in organic solvents, NMR studies were performed on monomers **1** and **2** as a model for the prepared polymer. In the ^1H NMR studies, we found that chemical shift of the NH of the leucine-terthiophenes shifted upon hydrogen bond formation. Furthermore, the ^{13}C chemical shift of the carbonyl acid also shifted downfield after imidazole addition. Further investigations: (i) characterization of the chiral electrode surface using different analytical techniques such as AFM and XPS, (ii) interactions of these chiral electrodes with other biomolecules such as enzymes, and (iii) modelling of the chiral surface in order to quantify the number of chiral centers at the surface are underway.

Acknowledgements

MC thanks the Natural Science and Engineering Research Council of Canada (NSERC) and Laurentian University for supporting this work. We also thank Dr J. Shepherd (measurements of the capacitive current) and Dr J. Gray-Munro (ATR-FTIR measurements) for their help.

Notes and references

1 M. M. Maye, D. Nykypanchuk, D. van der Lelie and O. Gang, *J. Am. Chem. Soc.*, 2006, **128**, 14020.
2 S. M. Schreiner, A. L. Hatch, D. F. Shudy, D. R. Howard, C. Howell, J. Zhao, P. Koelsch, M. Zharnikov, D. Y. Petrovykh and A. Opdahl, *Anal. Chem.*, 2011, **83**, 4288.
3 K. Ataka, F. Giess, W. Knoll, R. Naumann, S. Haber-Pohlmeier, B. Richter and J. Heberle, *J. Am. Chem. Soc.*, 2004, **126**, 16199.
4 J. Kim, J. Cho, P. M. Seidler, N. E. Kurland and V. K. Yadavalli, *Langmuir*, 2010, **26**, 2599.
5 S. Shunsuke, N. Tomoyasu, K. Masaharu, M. Toshihisa, D. Takehisa, O. Tsuyoshi, Y. Hisanori, I. Shigeru, H. Hideki and N. Mamoru, *Langmuir*, 2013, **29**, 5104.
6 C. Fang, H. Ji, W. Y. Karen and S. R. M. Rafei, *Biosens. Bioelectron.*, 2011, **26**, 2670.
7 C. Gutiérrez-Sánchez, D. Olea, M. Marques, V. M. Fernández, I. A. C. Pereira, M. Vélez and A. L. De Lacey, *Langmuir*, 2011, **27**, 6449.
8 J. J. Gooding, F. Mearns, W. R. Yang and J. Q. Liu, *Electroanalysis*, 2003, **15**, 81.
9 E. Huang, F. Zhou and L. Deng, *Langmuir*, 2000, **16**, 3272.
10 R. Singhvi, A. Kumar, Z. P. Lopez, G. N. Stephanopolous, D. I. Wang, G. M. Whitesides and D. E. Ingber, *Science*, 1994, **264**, 696.
11 M. Bhuvana, J. S. Narayanan, V. Dharuman, W. Teng, J. H. Hahn and K. Jayakumar, *Biosens. Bioelectron.*, 2013, **41**, 802.
12 D. W. Hatchett and M. Josowicz, *Chem. Rev.*, 2008, **108**, 746.
13 N. Meyerbröker, Z.-A. Li, W. Eck and M. Zharnikov, *Chem. Mater.*, 2012, **24**, 2965.

14 A. Ulman, *Chem. Rev.*, 1996, **96**, 1533.
15 C. D. Bain, H. A. Biebuyck and G. M. Whitesides, *Langmuir*, 1989, **5**, 723.
16 J. T. Young, F. J. Boerio, Z. Zhang and T. L. Beck, *Langmuir*, 1996, **12**, 1219.
17 T. K. Herne and M. J. Tarlov, *J. Am. Chem. Soc.*, 1997, **119**, 8916.
18 S. O. Kelley, J. K. Barton, N. M. Jackson, L. D. McPherson, A. B. Potter, E. M. Spain, M. J. Allen and M. G. Hill, *Langmuir*, 1998, **14**, 6781.
19 M. Chahma, J. S. Lee and H.-B. Kraatz, *J. Electroanal. Chem.*, 2004, **567**, 283.
20 G. Hager and A. G. Brolo, *J. Electroanal. Chem.*, 2003, **550–551**, 291.
21 A. Houmam, H. Muhammad, M. Chahma, K. Koczkur and D. F. Thomas, *Chem. Commun.*, 2011, **47**, 7095.
22 H. Muhammad, K. M. Koczkur, A. H. Kycia and A. Houmam, *Langmuir*, 2012, **28**, 15853.
23 D. J. Garrett, J. Lehr, G. M. Miskelly and A. J. Downard, *J. Am. Chem. Soc.*, 2007, **129**, 15456.
24 S. Baranton and D. Bélanger, *J. Phys. Chem. B*, 2005, **109**, 24401.
25 A. Adenier, C. Combellas, F. Kanoufi, J. Pinson and F. I. Podvorica, *Chem. Mater.*, 2006, **18**, 2021.
26 C. Combellas, F. Kanoufi, J. Pinson and F. I. Podvorica, *J. Am. Chem. Soc.*, 2008, **130**, 8576.
27 A. J. Downard, *Electroanalysis*, 2000, **12**, 1085.
28 X. Li, Y. Wan and C. Sun, *J. Electroanal. Chem.*, 2004, **569**, 79.
29 J. Heinze, B. A. Frontana-Uribe and S. Ludwigs, *Chem. Rev.*, 2010, **110**, 4724.
30 S. Komathi, A. I. Gopalan, S.-K. Kim, G. S. Anand and K.-P. Lee, *Electrochim. Acta*, 2013, **92**, 71.
31 M. A. Rahman, N.-H. Kwon, M.-S. Won, E. S. Choe and Y.-B. Shim, *Anal. Chem.*, 2005, **77**, 4854.
32 M. Wilchek and E. A. Bayer, *Anal. Biochem.*, 1988, **171**, 1.
33 H. Mehenni, *Can. J. Chem.*, 2012, **90**, 271.
34 F. Mouffouk and S. J. Higgins, *Electrochem. Commun.*, 2006, **8**, 15.
35 P. Pellon, E. Deltel and J.-F. Pilard, *Tetrahedron Lett.*, 2001, **42**, 867.
36 C. R. G. Grenier, S. J. George, T. J. Joncheray, E. W. Meijer and J. R. Reynolds, *J. Am. Chem. Soc.*, 2007, **129**, 10694.
37 K. P. R. Nilsson, M. R. Andersson and O. Inganas, *Synth. Met.*, 2003, **135–136**, 291.
38 K. P. R. Nilsson, D. Johan, J. D. Olsson, P. Konradsson and O. Inganas, *Macromolecules*, 2004, **37**, 6316.
39 K. P. R. Nilsson, J. D. Olsson, F. Stabo-Eeg, M. Lindgren, P. Konradsson and O. Inganas, *Macromolecules*, 2005, **38**, 6813.
40 F. Tassinari, S. P. Mathew, C. Fontanesi, L. Schenetti and R. Naaman, *Langmuir*, 2014, **30**, 4838.
41 A. Mucci, F. Parenti and L. Shenetti, *Macromol. Rapid Commun.*, 2003, **24**, 547.
42 K. P. Nilsson, J. Rydberg, L. Baltzer and O. Inganäs, *Proc. Natl. Acad. Sci. U. S. A.*, 2003, **100**, 10170.
43 A. Åslund, A. Herland, P. Hammarström, K. P. R. Nilsson, B.-H. Jonsson, O. Inganäs and P. Konradsson, *Bioconjugate Chem.*, 2007, **18**, 1860.
44 C. D. McTiernan and M. Chahma, *New J. Chem.*, 2010, **34**, 1417.
45 C. D. McTiernan and M. Chahma, *Synth. Met.*, 2011, **161**, 1532.
46 C. D. McTiernan, S. Abbas and M. Chahma, *New J. Chem.*, 2012, **36**, 2106.
47 G. B. Thomas and R. L. Finney, *Calculus and Analytic Geometry*, Addison Wesley, 9th edn, 1996.
48 C. D. McTiernan, K. Omri and M. Chahma, *J. Org. Chem.*, 2010, **75**, 6096.
49 M. Chahma, D. J. T. Myles and R. G. Hicks, *Macromolecules*, 2004, **37**, 2010.
50 M. Chahma, D. J. T. Myles and R. G. Hicks, *Chem. Mater.*, 2005, **17**, 2672.
51 L. Groenendaal, F. Jonas, D. Freitag, H. Pielartzik and J. R. Reynolds, *Adv. Mater.*, 2000, **12**, 481.
52 A. J. Bard and L. R. Faulkner, *Electrochemical Methods. Fundamentals and Applications*, Wiley, New York, 2nd edn, 2001.
53 A. Emge and P. Bäuerle, *Synth. Met.*, 1999, **102**, 1370.
54 P. Bäuerle and A. Emge, *Adv. Mater.*, 1998, **10**, 324.
55 A. M. Lesk, *Introduction to protein architecture*, Oxford University Press, Oxford, 2001.
56 A. Scott and J. E. Gray-Munro, *Thin Solid Films*, 2009, **517**, 6809.
57 J. W. Keller, *J. Phys. Chem. A*, 2004, **108**, 4610.
58 M. Pohjakallio, G. Sundholm and P. Talonen, *J. Electroanal. Chem.*, 1996, **406**, 165.
59 E. N. Nikolova, F. L. Gottardo and H. M. Al-Hashimi, *J. Am. Chem. Soc.*, 2012, **134**, 3667.
60 T. Nakano and Y. Masuda, *J. Phys. Chem. A*, 2012, **116**, 8409.
61 S. Zheng, Q. Guo and C. M. Chan, *J. Polym. Sci., Part B: Polym. Phys.*, 2003, **41**, 1099.